

Synthesis of Titanium Dioxide Nanotubes with Different N-Containing Ligands via Hydrothermal Method

Cheng Yee Leong¹, Ye Shen Lo¹, Pei Wen Koh², Siew Ling Lee^{1,3*}

¹Department of Chemistry, Faculty of Science, Universiti Teknologi Malaysia, 81310 Johor Bahru, Malaysia

²CSC Screen Process Supplies Sdn Bhd, 14, Jalan Bertam 5, Taman Daya, 81100 Johor Bahru, Johor, Malaysia

³Centre for Sustainable Nanomaterials, Ibnu Sina Institute for Scientific and Industrial Research, Universiti Teknologi Malaysia (UTM), 81300 Johor Bahru, Malaysia

*Corresponding author: lsling@utm.my

Abstract

Titanium dioxide (TiO_2) nanotubes (TNT) were successfully synthesized using different N-containing ligands via hydrothermal method. Methylamine, ethylenediamine and diethylenetriamine with different Ti/ligand molar ratios (1:1, 1:3, 1:5 and 1:8) were prepared. As-synthesized TiO_2 without N-containing ligands were also prepared for comparison purpose. The X-Ray Diffraction patterns confirmed the presence of anatase phase of TiO_2 in all the synthesized samples whereas the presence of sodium titanate was only detected in the samples containing N-containing ligands. The Transmission Electron Microscopy images also showed that the N-containing ligands promoted the formation of nanotubes in the anatase TiO_2 . Based on the Tauc Plot, the band gap energy of anatase TiO_2 was shifted with the addition of methylamine, ethylenediamine and diethylenetriamine. The photoluminescence spectra also showed that with the addition of sufficient amount of N-containing ligands, the intensity of photoluminescence spectrum decreased, suggesting formation of more nanotube and reduction of electron hole recombination rate. The photocatalytic performance of all synthesized samples was determined through photodegradation of Congo red under UV light for 6 hours. The results suggested that among the synthesized materials, the sample which contained diethylenetriamine with molar ratio of 5 gave the highest photocatalytic activity of 76.71% which could be attributed to successful formation of nanotube, its higher surface reaction rate and low electron hole recombination. Diethylenetriamine showed higher efficiency in assisting the formation of TiO_2 nanotubes compared to methylamine and ethylenediamine.

Keywords

Titanium dioxide nanotube, N-containing ligands, photocatalyst, hydrothermal, Congo red

Received: 20 February 2021, Accepted: 23 March 2021

<https://doi.org/10.26554/sti.2021.6.2.67-73>

1. INTRODUCTION

Titanium dioxide (TiO_2) nanoparticles is examined as an inert and safe material and has been used in many applications such as pigments, sunscreen and coloring. Nonetheless, TiO_2 only absorbs ultraviolet light due to its large band gap energy of 3.2 eV. Therefore, it is desirable to reduce the band gap of anatase TiO_2 to be active under visible region. Several approaches had been used including doping of metal and non-metal as well as modification of the surfaces (Koh et al., 2017; Ooi et al., 2020; Ooi et al., 2016; Lee et al., 2016). Doping of TiO_2 with metals has a major drawback that the photocatalytic activity of metal doped TiO_2 could be influenced by dopant concentration. While, for the doping of TiO_2 with non-metals, the doping into the lattice of TiO_2 usually resulted in the formation of oxygen vacancies in the bulk which deteriorate the visible light photocatalysis efficiency in industrial applications

(Dong et al., 2011; Li et al., 2008). As an alternative, the morphologies of TiO_2 photocatalysts has been intensively explored to improve its performance as a photocatalyst. Compared to zero-dimensional and two-dimensional nanostructures, more attention has been paid to one-dimensional TiO_2 nanostructures which include nanowire, nanorod and nanotube due to its high aspect ratio, large specific surface area and excellent ionic charge transport property (Lee et al., 2014).

Hydrothermal synthesis is a facile and preferable route for the synthesis of TiO_2 nanotubes since the products prepared by this method have well crystalline phase, which benefits to thermal stability of the nanosized materials. Even so, traditional hydrothermal synthesis of TiO_2 nanotubes often requires highly concentrated alkali such as 10 to 12 M of KOH or NaOH (Kasuga et al., 1998). In our research group's previous study, it showed that the synthesis of TiO_2 nanotubes could be done in the presence of low concentration of alkali with the assistance

of N-ligand (Leong et al., 2020). In that study, methylamine was used as the N-ligand, allowing the binding between the N atom of methylamine with the Ti_4^+ of the titanate layer, hence, assisting the nanosheet to curl up, forming TiO_2 nanotube (Leong et al., 2020). Other than methylamine, both the ethylenediamine and diethylenetriamine (DETA) are also the N-ligands. More N atoms can be found in these two N-ligands as compared to methylamine. Since the N atom plays a major role in assisting the TiO_2 nanotubes formation as proven in the previous study, it is expected that ethylenediamine and DETA work better than methylamine. As such, this current study is aimed to investigate the effect of different N-containing ligands on the formation of TiO_2 . An attempt was made to synthesize TiO_2 nanotubes with different N-containing ligands via hydrothermal method in a fixed hydrothermal condition.

2. EXPERIMENTAL SECTION

2.1 Materials

Anatase TiO_2 powder (Sigma Aldrich, $\geq 99.0\%$), methylamine hydrochloride (Sigma Aldrich, $\geq 98.0\%$), ethylenediamine (Merck, $\geq 99.0\%$), diethylenetriamine (Merck, $\geq 98.0\%$), sodium hydroxide (Merck, $\geq 99.0\%$), Congo red.

2.2 Methods

In a typical synthesis, inside a Teflon bottle, 0.5 g of anatase TiO_2 powder was mixed with mixture of 70 mL of 7 M sodium hydroxide and 0.419 mL ethylenediamine. The molar ratio of Ti to ethylenediamine was 1:1. The mixture was stirrer vigorously (1000 rpm) for 1 h. After that, the Teflon bottle was transferred into stainless-steel autoclave and hydrothermally treated at 130°C for 24 h. The obtained white precipitate was washed with 0.01 M sulfuric acid and double distilled water until pH 7 before drying at 60°C overnight. Samples with other Ti to ethylenediamine molar ratio (1:3, 1:5, 1:8) was prepared with the same conditions. Samples were also prepared with exactly the same method and conditions using methylamine and diethylenetriamine as the ligand in replacement of ethylenediamine. For comparison purpose, as- TiO_2 was prepared with the same conditions without addition of ethylenediamine. Samples was labelled as xY-TNT where x is the molar ratio of ligand (1,3,5,8), Y is the ligand (methylamine, ethylenediamine, diethylenetriamine) and TNT is the titania nanotube.

The phases and crystallinity of the samples were examined with X-ray Diffractometer (XRD) (Bruker Advance D8) with $\text{Cu K}\alpha$ irradiation ($\lambda = 0.15406 \text{ nm}$, 40 KV, 40 mA). Samples were scanned in the range $2\theta = 2 - 80^\circ$ with step size $0.05^\circ/\text{s}$. The morphology of the selected samples was confirmed with Transmission Electron Microscopy (TEM) (JEOL JEM-2100) operating at 200 KV. Samples were dispersed in absolute ethanol and ultrasonicated for 10 minutes prior to load onto carbon coated copper grid. (Perkin Elmer Ultraviolet-visible Spectrometer Lambda 35) was used to study the optical properties of the samples. Barium sulphate was used as the reference. Fixed amount of sample ($2.000 \pm 0.0005 \text{ g}$) was put

into the sample holder and was scanned in the range $200 - 800 \text{ nm}$. Band gap energy of the samples was obtained from Tauc plot. It is a plot of $(\alpha h\nu)^2$ against $h\nu$ where α is the absorbance, h is the Planck constant and ν is the velocity of light. Photoluminescence (JASCO, FP-8500) with an excitation of 344 nm was used to study the rate of electron-hole recombination of the samples.

Photocatalytic testing was carried out using 50 mL 15 ppm Congo red and 0.01 g samples and irradiated under UV for 6 h. Prior to reaction, adsorption was carried out to ensure the decreased of the concentration was attributed solely to photodegradation.

3. RESULTS AND DISCUSSION

3.1 Structural Properties

Figure 1 illustrated the XRD patterns of as-synthesized TiO_2 and samples different N-ligands molar ratio. The XRD pattern of as-synthesized TiO_2 pattern confirmed the presence of anatase phase (JCPDS 21-1272) in which the peaks can be found at 2θ values of $24.8^\circ, 37.3^\circ, 47.6^\circ, 53.5^\circ, 55.1^\circ$ and 62.2° that corresponded to (101), (004), (200), (105), (211) and (204) crystal planes respectively. The peak positions were consistent with the standard diffraction pattern of anatase TiO_2 with no other crystalline phase observed. A broad peak was observed at 2θ values of 28° in the synthesized samples that containing N-ligands. The peak represented $\text{Na}_2\text{Ti}_3\text{O}_7$ type of sodium titanate (JCPDS 31-1329). The presence of Na atoms can be explained when treating the raw material with aqueous NaOH solution, some Ti-O-Ti bonds were broken, and Ti-O-Na and Ti-OH bonds were formed (Kasuga et al., 1998). It was proposed that acid treatment on the sample changed the composition in the sample from sodium titanate to hydrogen titanate through an ion exchange mechanism and affected the attributes of TNTs owing to the relative amount of Na and H atoms within TNT structure (OU and LO, 2007). However, there were not characteristic peak of hydrogen titanate observed in the XRD pattern. It was because the pH of the samples were washed approximately to 7 that can retard the ion exchange process so the nanotubes mostly retain their sodium titanate composition (Weng et al., 2006).

3.2 Morphology of the Samples

Figure 2 showed the TEM and HRTEM images of the selected samples. A mixture of unreacted nanoparticles of TiO_2 powders and TiO_2 nanotubes was observed in Figure 2 (e) and (f). The nanoparticles of TiO_2 in anatase had a spherical morphology. From the distance between the adjacent lattice fringes, the nanoparticles showed lattice spacing of $d = 0.35 \text{ nm}$ for the (101) plane of the anatase phase which was consistent with the XRD results. Figure 2 (a), (b), (c) and (d) showed the TEM micrograph of the samples that contained N-ligands. It can be observed that the samples both contained TiO_2 nanotubes that overlap each other and had constant diameter of 10 - 15 nm. The interspacing between the neighboring anatase of the tube

Table 1. Synthesis Conditions of Different Ligands with Different Ratio

Ligand	Ratio	Volume (mL) / Weight used (g)	Temperature (°C)	Duration (Hours)	Label
Methylamine	1:01	0.0972 g	130	24	1 MT TNT
Methylamine	1:03	0.5833 g	130	24	3 MT TNT
Methylamine	1:05	0.9721 g	130	24	5 MT TNT
Methylamine	1:08	1.5553 g	130	24	8 MT TNT
Ethylenediamine	1:01	0.4190 mL	130	24	1 ET TNT
Ethylenediamine	1:03	1.2580 mL	130	24	3 ET TNT
Ethylenediamine	1:05	2.0970 mL	130	24	5 ET TNT
Ethylenediamine	1:08	3.8550 mL	130	24	8 ET TNT
Diethylenetriamine	1:01	0.6458 mL	130	24	1 DT TNT
Diethylenetriamine	1:03	1.9375 mL	130	24	3 DT TNT
Diethylenetriamine	1:05	3.2290 mL	130	24	5 DT TNT
Diethylenetriamine	1:08	5.1668 mL	130	24	8 DT TNT

wall was determined to be about 0.24 nm which correspond for the plane (004) of anatase TiO₂.

Scherrer Equation was then used to calculate the crystallite size of as-synthesized TiO₂ and samples that contained N-ligands. From the calculation, the crystallite size of as-synthesized was larger than samples that contained N-ligands. It was reported that smaller crystallite size of TiO₂ with high surface area can increase the number of active surface sites and the surface charge carrier transfer rate in the photocatalytic reaction (Carrera-López and Castillo-Cervantes, 2012). The results indicated that as-synthesized TNT has crystallite size of 31.60 nm. Upon modification with either methylamine, ethylamine or diethylenetriamine surfactant, the crystallite size of the samples decreased to the range of 26.33 – 26.27 nm. This showed that the addition of these three surfactants able to reduce the crystallite size of TNT. However, comparison among the modified samples, it was noted that the amount of surfactant has insignificant effect on the crystallite size. This was because N atoms had been introduced into the lattice without changing the average unit cell dimension (Sathish et al., 2005).

3.3 Optical Properties

In order to study the effect of diethylenetriamine ligand towards the optical property of TiO₂ NT, the synthesized samples were subjected to analysis using DR-UV-Vis spectrophotometer. The optical spectrum of the samples was depicted in Figure 3.

As shown in Figure 3 (a), it had a peak located between range of 270 nm to 280 nm, which were associated with the hydrated tetrahedral Ti species that is widely recognized as the most important Ti species to provide active site for the photocatalytic activity of TiO₂ (Lee et al., 2015; Xu et al., 2015). The band gap energy was determined using Tauc Plot, the addition of diethylenetriamine increased the band gap energy of as-synthesized TiO₂ NT from 3.2 eV to 3.25 eV, 3.27

eV, 3.29 eV and 3.31 eV for 1 DT TNT, 3 DT TNT, 5 DT TNT and 8 DT TNT respectively. Apparently, the band gap energy increased when the molar ratio of diethylenetriamine increased. It was reported that the decrease in particle size resulted in increased of band gap energy due to quantum size effect (Avinash et al., 2016). As shown in Figure 3 (b), TNT synthesized with the presence of ethylenediamine gave a similar optical spectrum when diethylenetriamine was used; there was broad peak located between range of 280 nm to 295 nm which was attributed to octahedral Ti (Lee et al., 2015). The addition of ethylenediamine decreased the band gap energy of as-synthesized TiO₂ NT from 3.2 eV to 2.95 eV, 2.93 eV, 3.03 eV and 3.13 eV for 1 ET TNT, 3 ET TNT, 5 ET TNT and 8 ET TNT respectively.

In general, addition of ethylamine surfactant reduced the band gap energy of as-synthesized TiO₂ from UV region to visible light region. This visible light absorption could be attributed to the N atom of the surfactant which nitrogen was incorporated in TiO₂ lattice so the localized N 2p states were positioned above the titanium dioxide valence band and the band gap became narrow (Dolat et al., 2013). As shown in Figure 3 (c), an absorption peak at 320 nm was indicated in all synthesized samples except as-synthesized TiO₂ which was associated to anatase TiO₂ (Xiong et al., 2017). An absorption peak at 270 nm can be found in all synthesized samples which was related to amorphous Ti (Camblor et al., 1993). It could be suggested that methylamine promoted the transformation of amorphous Ti species crystalline anatase phase of TiO₂. The addition of methylamine increased the band gap energy of as-synthesized TiO₂ NT from 3.2 eV to 3.37 eV, 3.41 eV, 3.35 eV and 3.27 eV for 1 MT TNT, 3 MT TNT, 5 MT TNT and 8 MT TNT respectively. There was no significant influence of the molar ratio of methylamine on the band gap energy of TiO₂. The increase of band gap energy of samples synthesized

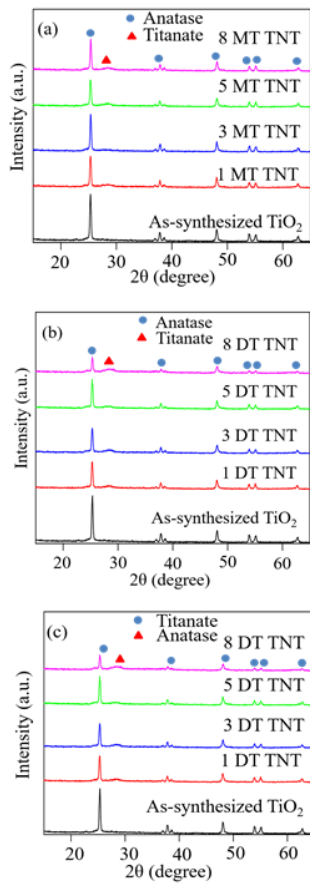


Figure 1. XRD Patterns of (a) Samples with Methylamine and As-synthesized TiO_2 , (b) Samples with Ethylenediamine and As-synthesized TiO_2 , (c) Samples with Diethylenetriamine and As-synthesized TiO_2

with the presence of methylamine compared to as-synthesized TiO_2 TNT could be due to quantum size effect (Avinash et al., 2016).

3.4 Photoluminescence Study

Photoluminescence spectroscopy was carried out to study the electron hole recombination rate. From Figure 4 (a), the intensity did not directly relate to the molar ratio of diethylenetriamine. 1 DT TNT has the highest intensity while 8 DT TNT has the lowest emission intensity. The results implied that 1 DT TNT had the lowest electron-hole recombination rate while 8 DT TNT had the highest electron-hole recombination rate.

Compare to as-synthesized TiO_2 , except 8 DT TNT, presence of diethylenetriamine reduced the electron-hole recombination rate of as-synthesized TiO_2 TNT which could be attributed to diethylenetriamine assisted in formation of nanotube.

It was reported that nanotube enhanced the electron transfer to the surface hence retard the electron-hole recombination

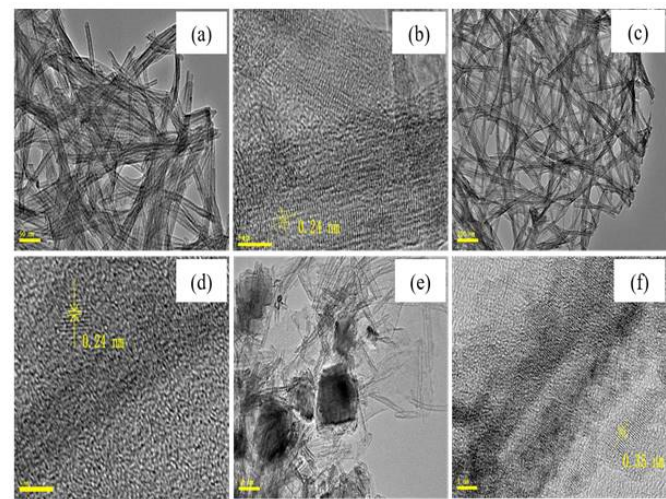


Figure 2. TEM and HRTEM Image of (a), (b) 5 DT TNT, (c), (d) 3 MT TNT, and (e), (f) as-synthesized TiO_2

rate (Sun et al., 2008). Addition of excess surfactant ($\text{Ti:DETA} = 1:8$) resulted in increasing of electron-hole recombination rate. This could be due to excess of surfactant acted as recombination center. From Figure 4 (b), the lowest intensity of the peak was 1 ET TNT and the highest intensity of the peak was 8 ET TNT. The intensity of the peak of 1 ET TNT was lower compared to as-synthesized TiO_2 could be attributed to more nanotube was formed which retarded the electron-hole recombination rate (Sun et al., 2008).

On the other hand, further addition of diethylenediamine increased the emission intensity even though more nanotube was formed. A possible explanation for increased emission intensity could be ascribed to more electrons were excited from valance band to conduction band (Fang et al., 2015). From Figure 4 (c), there was a decrease in fluorescence intensity with an increase in the amount of methylamine added to the anatase TiO_2 . It can be explained that the formation of more nanotube as evidence from the TEM images, reduced the electron-hole recombination rate. Alternatively, the nitrogen facilitated the separation of photo-generated electron–hole pair for the formation of oxygen vacancies that can inhibit the recombination of photo-generated charge to some extent (Irie et al., 2003). The intensity for 5 MT TNT was exactly the same 8 MT TNT. This indicated that the reduction in photoluminescence intensity had achieved saturation without further reduction. From Figure 4 (d), 3 MT TNT had the lowest intensity which indicated it had lowest electron hole recombination rate but it can decrease the surface reaction rate and lower the photocatalytic activity (Wojcieszak et al., 2013).

3.5 Photocatalytic Testing

From Table 2, the photocatalytic activity for 5 DT TNT was higher compared to as-synthesized TiO_2 . It can be explained based on the TEM micrographs in which more TiO_2 nanotubes

Table 2. Photocatalytic Activities of Samples Prepared with and without Diethylenetriamine

Temperature (°C)	Duration (hours)	Sample	Q ₁ (ppm)	Q ₂ (ppm)	Photocatalytic Efficiency (%)
130	24	As-synthesized TiO ₂	12.9	5.91	54.2
130	24	1 DT TNT	12.76	5.16	59.6
130	24	3 DT TNT	13.26	4.94	62.7
130	24	5 DT TNT	13.29	3.1	76.7
130	24	8 DT TNT	12.98	4.79	63.1

Table 3. Photocatalytic Activities of Samples Prepared with and without Ethylenediamine

Temperature (°C)	Duration (hours)	Sample	Q ₁ (ppm)	Q ₂ (ppm)	Photocatalytic Efficiency (%)
130	24	As-synthesized TiO ₂	12.9	5.91	54.2
130	24	1 ET TNT	13.68	6.87	49.8
130	24	3 ET TNT	13.43	5.96	55.6
130	24	5 ET TNT	12.62	3.61	71.4
130	24	8 ET TNT	12.16	6.9	43.2

were produced with the addition of diethylenetriamine compared to as-synthesized TiO₂. Diethylenetriamine might assist the scrolling of the intermediate nanosheet to form nanotube in which higher degree of nanotubes formation enhanced the photocatalytic activity of TiO₂.

Besides, the results showed that the photocatalytic efficiency increased when the molar ratio of diethylenetriamine increased until a certain extent. This is because appropriate amount of diethylenetriamine and appropriate temperature were beneficial to increase excited electrons, and thus improve the photocatalytic activity. Even though 5 DT TNT did not have the lowest electron-hole recombination rate (it has the second lowest emission intensity as shown in the photoluminescence spectra in Figure 4 (a)), but it has the best photocatalytic activity. This could be because it had faster surface reaction rate than the recombination rate that resulted in a net increase of photocatalytic efficiency. It was reported that both recombination rate and surface reaction rate were the factors to determine the photocatalytic activity.

From Table 3, subsequent increase of molar ratio of ethylenediamine from 1 to 5, the photocatalytic activity of TiO₂ nanotubes was increased. 5 ET TNT has the highest photocatalytic efficiency of 71.4%. Even though 5 ET TNT has relatively higher emission intensity compared to 1 ET TNT and 3 ET TNT, but the obtained photocatalytic efficiency was higher than the later. The reason could be the surface reaction rate at 5 ET TNT was very high which overcome the effect of electron-hole recombination and resulted in a better activity. On the other hand, the photocatalytic activity decreased after the ethylenediamine molar ratio used was higher than 5. This could be deduced that addition of excess ethylenediamine acted as recombination centre and the fate of electron-hole recombin-

ation rate was more prevailed. From Table 4, samples contained methylamine had higher photocatalytic activity compared to as-synthesized TiO₂ and 3 MT TNT had the highest photocatalytic efficiency.

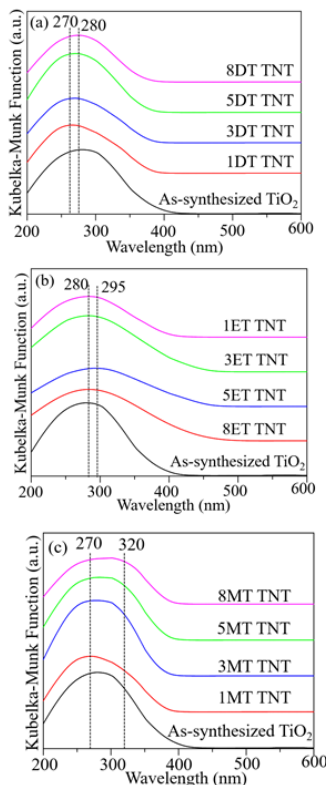
From the TEM micrograph, the crystallite size of as-synthesized TiO₂ was larger than 3 MT TNT. It was reported that the average diffusion path length of charge carrier from the bulk to the surface became longer in a bigger TiO₂, which will result in deep trapping of charge carriers, leading to lower photocatalytic activity. In addition, reduction in crystallite size which resulted in larger surface area can increase the available surface-active sites and consequently resulting in higher photocatalytic efficiency. Therefore, it was believed that 3 MT TNT has the highest photocatalytic activity was attributed smaller crystallite size that resulted in faster charge transfer and more surface-active site.

4. CONCLUSIONS

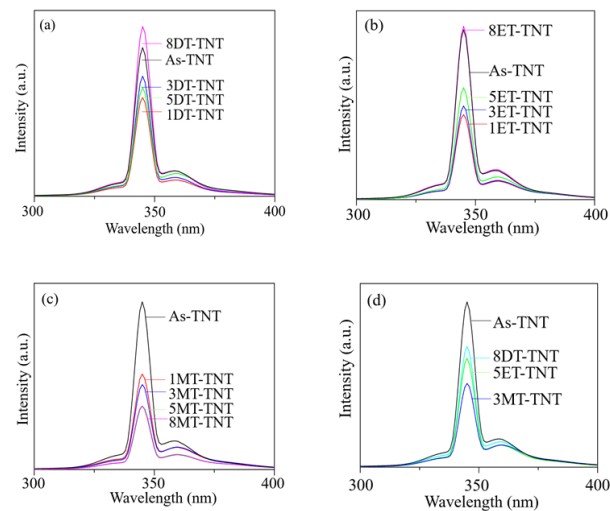
The synthesis of TiO₂ nanotubes were successfully performed via hydrothermal method using of different N ligands. All the samples consisted of white powder which indicated that the addition of N ligands did not affect the color of TiO₂. The samples were characterized successfully to study their physical and chemical properties. The XRD analysis indicated the presence of anatase TiO₂ and sodium titanate in the samples that contained N ligands. From the TEM analysis, more nanotubes were formed in 3 MT TNT and 5 DT TNT compared to as-synthesized TiO₂. From the Tauc plots, there was a shifting in the band gap energy of the samples that contained N ligands. Photoluminescence spectrum also showed there was a decrease in the intensity from the spectrum with the addition of certain N ligand until certain extent which can relate to the

Table 4. Photocatalytic Activities of Samples Prepared with and without Methylamine

Temperature (°C)	Duration (hours)	Sample	Q ₁ (ppm)	Q ₂ (ppm)	Photocatalytic Efficiency (%)
130	24	As-synthesized TiO ₂	12.9	5.91	54.2
130	24	1 MT TNT	13.07	4.16	68.2
130	24	3 MT TNT	12.82	3.93	69.4
130	24	5 MT TNT	13.27	5.24	60.5
130	24	8 MT TNT	12.67	5.26	58.45

**Figure 3.** DR-UV-Vis Spectra of (a) Methylamine, (b) Ethylenediamine, and (c) Diethylenetriamine

electron hole recombination rate. The photodegradation of Congo red also gave result that samples with N ligands with optimum molar ratio had higher photocatalytic activity than as-synthesized TiO₂. The photocatalytic efficiency for each of the synthesized samples was determined through photodegradation of Congo red under dark condition and UV irradiation for 6 hours. From the results, 5 DT TNT (76.7%), 5 ET TNT (71.4%) and 3 MT TNT (69.4%) showed the highest photocatalytic efficiency among their series and had higher photocatalytic efficiency than as-synthesized TiO₂ (54.2%). In conclusion, titanium dioxide nanotube was successfully synthesized via hydrothermal method in this study. 5 DT TNT was the best photocatalyst in the photodegradation of Congo red with photocatalytic activity of 76.71%. Methylamine, ethylene-

**Figure 4.** Photoluminescence Spectra of Titania Nanotube Synthesized with (a) Diethylenetriamine, (b) Ethylenediamine, (c) Methylamine, and (d) Comparison of Selected Samples with Highest Activities

diamine and diethylenetriamine played an important role to assist in the formation TiO₂ nanotube. Diethylenetriamine showed higher efficiency in assisting the formation of TiO₂ nanotubes compared to methylamine and ethylenediamine.

5. ACKNOWLEDGEMENT

Authors are whole-heartedly appreciated the financial support given by Ministry of Higher Education, Malaysia (MOHE) for the Fundamental Research Grant Scheme (Reference no.: FRGS/ 1/2019/STG07/UTM/02/12).

REFERENCES

- Avinash, B. S., V. S. Chaturmukha, H. S. Jayanna, C. S. Naveen, M. P. Rajeeva, B. M. Harish, S. Suresh, and A. R. Lamani (2016). Effect of particle size on band gap and DC electrical conductivity of TiO₂ nanomaterial. *AIP Conference Proceedings*, **1728**; 20426
- Camblor, M., A. Corma, and J. Pérez-Pariente (1993). Synthesis of titanoaluminosilicates isomorphous to zeolite Beta, active as oxidation catalysts. *Zeolites*, **13**(2); 82-87

- Carrera-López, R. and S. Castillo-Cervantes (2012). Effect of the phase composition and crystallite size of sol-gel TiO₂ nanoparticles on the acetaldehyde photodecomposition. *Surfaces y vacío*, **25**(2); 82–87
- Dolat, D., S. Mozia, B. Ohtani, and A. Morawski (2013). Nitrogen, iron-single modified (N-TiO₂, Fe-TiO₂) and co-modified (Fe, N-TiO₂) rutile titanium dioxide as visible-light active photocatalysts. *Chemical engineering journal*, **225**; 358–364
- Dong, F., S. Guo, H. Wang, X. Li, and Z. Wu (2011). Enhancement of the Visible Light Photocatalytic Activity of C-Doped TiO₂Nanomaterials Prepared by a Green Synthetic Approach. *The Journal of Physical Chemistry C*, **115**(27); 13285–13292
- Fang, Q., J. Tang, H. Zou, T. Cai, and Q. Deng (2015). Preparation of N-Doped Mesoporous TiO₂ Using Nitromethane as Nitrogen Source and Their High Photocatalytic Performance. *Synthesis and Reactivity in Inorganic, Metal-Organic, and Nano-Metal Chemistry*, **46**(5); 766–774
- Irie, H., Y. Watanabe, and K. Hashimoto (2003). Nitrogen-Concentration Dependence on Photocatalytic Activity of TiO₂-xNx Powders. *The Journal of Physical Chemistry B*, **107**(23); 5483–5486
- Kasuga, T., M. Hiramatsu, A. Hoson, T. Sekino, and K. Niihara (1998). Formation of Titanium Oxide Nanotube. *Langmuir*, **14**(12); 3160–3163
- Koh, P. W., M. H. M. Hatta, S. T. Ong, L. Yuliati, and S. L. Lee (2017). Photocatalytic degradation of photosensitizing and non-photosensitizing dyes over chromium doped titania photocatalysts under visible light. *Journal of Photochemistry and Photobiology A: Chemistry*, **332**; 215–223
- Lee, K., A. Mazare, and P. Schmuki (2014). One-Dimensional Titanium Dioxide Nanomaterials: Nanotubes. *Chemical Reviews*, **114**(19); 9385–9454
- Lee, S. L., J. M. Ekhsan, N. A. Kasiran, and A. A. Aziz (2015). Effect of Titania Loading on Properties and Catalytic Activity of Nanostructured Phosphate–Vanadia-Impregnated Silica–Titania Oxidative–Acidic Bifunctional Catalyst. *International Journal of Chemical Reactor Engineering*, **13**(1); 21–28
- Lee, S. L., S. P. Khaw, and Y. K. Ooi (2016). Vanadium oxides-doped porous titania photocatalysts for phenol photodegradation. *Malaysian Journal of Fundamental and Applied Sciences*, **12**(1); 28–33
- Leong, C. Y., P. W. Koh, Y. S. Lo, and S. L. Lee (2020). Hydrothermal synthesis of titanium dioxide nanotube with methylamine for photodegradation of Congo red. *IOP Conference Series: Materials Science and Engineering*, **833**; 012075
- Li, X., D. Wang, G. Cheng, Q. Luo, J. An, and Y. Wang (2008). Preparation of polyaniline-modified TiO₂ nanoparticles and their photocatalytic activity under visible light illumination. *Applied Catalysis B: Environmental*, **81**(3-4); 267–273
- Ooi, Y. K., M. H. M. Hatta, and S. L. Lee (2020). Properties and Photocatalytic Behaviour of Vanadia Loaded Titania Supported on MCM-41 Synthesized using Different Surfactants for Degradation of Methylene Blue. *Journal of the Indonesian Chemical Society*, **3**(1); 28–28
- Ooi, Y. K., L. Yuliati, and S. L. Lee (2016). Phenol photocatalytic degradation over mesoporous TUD-1-supported chromium oxide-doped titania photocatalyst. *Chinese Journal of Catalysis*, **37**(11); 1871–1881
- OU, H. and S. LO (2007). Review of titania nanotubes synthesized via the hydrothermal treatment: Fabrication, modification, and application. *Separation and Purification Technology*, **58**(1); 179–191
- Sathish, M., B. Viswanathan, R. P. Viswanath, and C. S. Gopinath (2005). Synthesis, Characterization, Electronic Structure, and Photocatalytic Activity of Nitrogen-Doped TiO₂Nanocatalyst. *Chemistry of Materials*, **17**(25); 6349–6353
- Sun, W.-T., Y. Yu, H.-Y. Pan, X.-F. Gao, Q. Chen, and L.-M. Peng (2008). CdS Quantum Dots Sensitized TiO₂Nanotube-Array Photoelectrodes. *Journal of the American Chemical Society*, **130**(4); 1124–1125
- Weng, L.-Q., S.-H. Song, S. Hodgson, A. Baker, and J. Yu (2006). Synthesis and characterisation of nanotubular titanates and titania. *Journal of the European Ceramic Society*, **26**(8); 1405–1409
- Wojcieszak, D., D. Kaczmarek, J. Domaradzki, and M. Mazur (2013). Correlation of Photocatalysis and Photoluminescence Effect in Relation to the Surface Properties of TiO₂:Tb Thin Films. *International Journal of Photoenergy*, **2013**; 1–9
- Xiong, G., Q. Jia, Y. Cao, L. Liu, and Z. Guo (2017). The effect of acid treatment on the active sites and reaction intermediates of the low-cost TS-1 in propylene epoxidation. *RSC Advances*, **7**(39); 24046–24054
- Xu, L., D.-D. Huang, C.-G. Li, X. Ji, S. Jin, Z. Feng, F. Xia, X. Li, F. Fan, C. Li, and P. Wu (2015). Construction of unique six-coordinated titanium species with an organic amine ligand in titanosilicate and their unprecedented high efficiency for alkene epoxidation. *Chemical Communications*, **51**(43); 9010–9013